



Gram–Charlier-Like Expansions of the Convoluted Hyperbolic-Secant Density

Federica Nicolussi¹ · Maria Grazia Zoia²

© Grace Scientific Publishing 2020

Abstract

Since financial series are usually heavy tailed and skewed, research has formerly considered well-known leptokurtic distributions to model these series and, recently, has focused on the technique of adjusting the moments of a probability law by using its orthogonal polynomials. This paper combines these approaches by modifying the moments of the convoluted hyperbolic secant. The resulting density is a Gram–Charlier-like (GC-like) expansion capable to account for skewness and excess kurtosis. Multivariate extensions of these expansions are obtained on an argument using spherical distributions. Both the univariate and multivariate (GC-like) expansions prove to be effective in modeling heavy-tailed series and computing risk measures.

Keywords Convoluted hyperbolic-secant distribution · Orthogonal polynomials · Kurtosis · Skewness · Gram–Charlier-like expansion

1 Introduction

A substantial body of evidence shows that empirical distributions of returns and financial data usually exhibit accentuated peakedness, thick tails and frequent skewness. This is duly acknowledged in the financial literature (see e.g., [42] orthogonal, and references therein). The well-known Gaussian law fails to accommodate these “stylized facts” and thus does not provide a valid paradigm for the representation and interpretation of financial data. This explains why research has moved toward leptokurtic distributions such as the Student- t , the Pearson type VII, the normal inverse Gaussian and stable distributions (see e.g., [35, 39]), which by and large maintain desirable properties like the bell-shapedness. Heavy tailed and peaked distributions

✉ Maria Grazia Zoia
maria.zoia@unicatt.it

¹ Department of Economics, Management and Quantitative Methods, Università degli Studi di Milano, Via Conservatorio, 7, Milan, Italy

² Department of Economic Policy, Università Cattolica del Sacro Cuore, Largo Gemelli, 1, Milan, Italy

have either been modeled by densities generated via a mixed approach (see e.g., [1, 2, 20]), or kernel estimators obtained by appropriate techniques (see [40]).

Other research has focused on mixtures of distributions built by combining a Gaussian density with a heavy-tailed generalized Pareto (GP) density. The former is intended to model the bulk of the observations of a series, the latter observations falling beyond a certain threshold, which can, or can not, be fixed in advance. The papers [8–10, 13, 18, 28, 31, 36, 37] provide contributions along these lines. To avoid mixtures that quickly inflate the number of parameters to estimate (see [33]), efforts have been made to generate GP-like random variables, either by replacing uniform draws in the probability integral transform with draws from other distributions, or by developing other types of extended GP's.

A different stream of research has recently come to the fore (see [21]). This is based on the idea of increasing the flexibility of a distribution by simply multiplying it by a nonnegative function and re-normalizing the product, thus obtained, to get a valid density. The choice of this multiplicative function, which should lead to a density with desirable features without introducing heavy computational burdens, represents the main hurdle of this approach. In this paper, we solve the problem by building a Gram–Charlier-like (GC-like) expansion of a leptokurtic distribution with the aim of obtaining a distribution capable of meeting the requirements of possibly severe kurtosis and skewness. A GCI expansion is obtained by multiplying a leptokurtic distribution by a function depending on a proper set of its own orthogonal polynomials. No re-normalization is needed as the resulting distribution turns out to be a density function with the required kurtosis and skewness. The approach here proposed can be viewed as an extension of the one hinging on Gram–Charlier expansions (GC in short), which is used to reshape the Gaussian law by using its own orthogonal polynomials which are Hermite polynomials (see [11, 26, 43]). GC-like expansions of leptokurtic distributions are proved to be more flexible distributions than the standard GC as the admissible value set of their moments is quite broader than that of GC laws. In this paper, we suggest reshaping a leptokurtic distribution, namely the convoluted hyperbolic-secant distribution, (CHS henceforth), which arises from the self-convolution of the hyperbolic secant (see e.g., [4, 6, 17]). In particular, we investigate the capacity of GC-like expansions of the CHS law to fit in with financial data. Furthermore, as risk modeling applications typically require that several variables are jointly modeled, a multivariate extension of both the CHS distribution and its orthogonal polynomial expansion are provided. The latter is easily derived from spherical distribution theory (see [15]).

Applications to financial univariate and multivariate asset returns, characterized by substantial excess kurtosis, prove the usefulness of this choice by highlighting the extent to which the polynomially adjusted convoluted hyperbolic-secant distribution matches up with empirical evidence. The goodness of the proposed distributions in computing some risk measures, like the value at risk and the expected shortfall, is shown.

The paper is organized as follows. In Sect. 2, we design the polynomial shape-adapter tailored to build GC-like expansions of a CHS law both for the univariate and multivariate contexts. In Sect. 3, the performance of these GC-like distributions is tested by an application involving both univariate and bivariate financial returns.

Section 4 draws the conclusions. An “Appendix,” providing the essentials on orthogonal polynomials, spherical distributions and computations concerning the maximum likelihood estimation of GC-like expansions, completes the paper.

2 Univariate and Multivariate Gram–Charlier-Like Expansions of the Convoluted Hyperbolic-Distribution

In this section, we will devise a GC-like expansion for the even CHS density

$$f(x) = x \left(\sin h \left(\frac{\pi}{\sqrt{2}} x \right) \right)^{-1} \quad x \in \mathbb{R}. \quad (1)$$

The CHS distribution, which is the self-convolution of the hyperbolic secant law and the Fourier image of the logistic function (see, e.g., [19]), enjoys several desirable properties like bell-shapedness, leptokurtosis and the existence of moments and orthogonal polynomials of every order. As far as even moments are concerned, they can be obtained from the following integral (see [23], p. 348, formula 3.523.2)

$$\int_0^\infty \frac{x^{2h-1}}{\sin h(bx)} dx = \frac{2^{2h} - 1}{2h} \left(\frac{\pi}{b} \right)^{2h} |B_{2h}|, \quad h = 1, 2, \dots \quad (2)$$

where B_{2h} denotes the $2h$ -th Bernoulli number. By setting $h = 1, 2, 3, 4, 5$ in (2) we obtain the first five even moments for this density

$$m_0 = 1, \quad m_2 = 1, \quad m_4 = 4, \quad m_6 = 34, \quad m_8 = 496. \quad (3)$$

These values can be used to determine the coefficients of the polynomial shape adapter of the GC-like expansions for the CHS distribution. The term GC-like expansion is adopted to indicate a density, $\tilde{g}(x, \alpha, \beta, \dots)$ hereafter, obtained by reshaping an arbitrary distribution $f(x)$ by using its own orthogonal polynomials that is polynomials with coefficients built from the moments of this law. The term can be traced back to the well-known Gram–Charlier (GC) expansion referred to the Gaussian law and Hermite polynomials. The GC-like expansion based on the j -th orthogonal polynomial $p_j(x)$ associated with a density $f(x)$ takes the form

$$\tilde{g}(x, \alpha) = q(x, \alpha) f(x). \quad (4)$$

Here, $q(x, \alpha) = \left(1 + \frac{\alpha}{\gamma_j} p_j(x) \right)$ is a shape adapter; its role is to increase the j -th moment of the density $f(x)$ by a quantity equal to α while γ_j is the squared norm of $p_j(x)$ (see “Appendix A1” for more details on orthogonal polynomials and GC-like expansions).

In what follows we will focus on GC-like expansions which make use of the third and fourth orthogonal polynomials of a given density $f(x)$ in order to account for skewness and excess kurtosis. The expansions at stake take the form

$$\tilde{g}(x, \alpha, \beta) = q(x, \alpha, \beta) f(x), \quad (5)$$

where $q(x, \alpha, \beta)$ is the trinomial

$$q(x, \alpha, \beta) = \left(1 + \frac{\alpha}{\gamma_3} p_3(x) + \frac{\beta}{\gamma_4} p_4(x) \right) \quad (6)$$

depending on the 3rd and 4th orthogonal polynomials, $p_3(x)$ and $p_4(x)$, associated with $f(x)$. The parameters α and β represent, respectively, the increase in skewness and kurtosis attainable with the polynomial expansion (5), while γ_3 and γ_4 are, respectively, the squared norms of $p_3(x)$ and $p_4(x)$ (see formula (63) in “Appendix A1”).

The following theorem shows how to compute the third and fourth degree orthogonal polynomials associated with CHS density which paves the way to obtaining the family of the GC-like expansion, as defined in (5) for this density.

Theorem 1 *The family of the GC-like expansions, as defined in (5) for the CHS density is given by*

$$\tilde{g}(x, \alpha, \beta) = \left(1 + \frac{\alpha}{18} p_3(x) + \frac{\beta}{180} p_4(x) \right) x \left(\sin h \left(\frac{\pi}{\sqrt{2}} x \right) \right)^{-1}, \quad (7)$$

where α and $\beta > 0$ are parameters and

$$p_3(x) = x^3 - 4x, \quad p_4(x) = x^4 - 10x^2 + 6 \quad (8)$$

are the third and fourth degree orthogonal polynomials associated with the CHS density. Under suitable conditions on α and β , formula (7) defines a set of densities with skewness and kurtosis different from those of the parent CHS density by an extent equal to α and β , respectively.

Proof As the CHS density is a symmetric law, its third and fourth-order orthogonal polynomials, $p_3(x)$ and $p_4(x)$, are specified as in (67) of “Appendix A1.” The coefficients of these polynomials and their squared norms, γ_3, γ_4 in the trinomial (6), are obtained from formulas (64) and (66) of “Appendix A1.” The proof that the skewness and kurtosis of the GC-like expansion in (7) are modified by a quantity equal to α and β respectively, is based on Theorem A1 in “Appendix A1.”

The positiveness of $q(x, \alpha, \beta)$ is mandatory in order for $\tilde{g}(x, \alpha, \beta)$ to be a density function. It is worth distinguishing the case in which only extra kurtosis has to be accounted for, from the case in which both excess kurtosis and skewness are at work. Let’s start with the former case. \square

Lemma 1 *For the binomial*

$$q(x, 0, \beta) = \left(1 + \frac{\beta}{180} (x^4 - 10x^2 + 6) \right) \quad (9)$$

to be nonnegative for all x , it is required that the parameter β satisfies

$$0 \leq \beta \leq \frac{180}{19}. \quad (10)$$

Proof The proof rests on the argument that $p_4(x) = x^4 - ex^2 + g$ is bounded from below that is

$$\inf_x p_4(x) = \left(\frac{4g - e^2}{4} \right) = -19. \quad (11)$$

This entails that $q(x, 0, \beta) = \left(1 + \frac{\beta}{r_4} (x^4 - ex^2 + g) \right)$ is nonnegative, provided

$$\beta \leq \frac{4\gamma_4}{(e^2 - 4g)}. \quad (12)$$

Since $q(x, 0, \beta)$ is not bounded from above, negative values of β are not allowed. \square

In light of the foregoing theorem, the GC-like expansions of the CHS density (GCCHS hereafter)

$$\tilde{g}(x, 0, \beta) = \left(1 + \frac{\beta}{180} p_4(x) \right) x \left(\sin h \left(\frac{\pi}{\sqrt{2}} x \right) \right)^{-1} \quad (13)$$

prove suitable to model data with kurtosis, K , varying in the range

$$4 \leq K \leq 13.4737. \quad (14)$$

As for the more general case, when both extra kurtosis and skewness are involved, we have

Lemma 2 *The trinomial*

$$q(x, \alpha, \beta) = 1 + \frac{\alpha}{18} p_3(x) + \frac{\beta}{180} p_4(x) \quad (15)$$

is positive for all x if the pair of parameters α, β satisfy

$$[(\lambda - 0, 8)^2 + 0, 84] \beta < 21, 6 \quad (16)$$

$$25 \left[\lambda \left(39 + \frac{810}{\beta} \right) - 49 \right]^2 - \left[40\lambda + 39 + \frac{540}{\beta} - 37 \right]^3 < 0, \quad (17)$$

where $\lambda = \frac{15\alpha^2}{2\beta^2} + 2$.

Proof The trinomial $q(x, \alpha, \beta)$ is a quartic

$$\frac{\beta}{180} x^4 + \frac{\alpha}{18} x^3 - \frac{\beta}{18} x^2 - \frac{2\alpha}{9} x + \frac{\beta}{30} + 1 \quad (18)$$

whose signature is the same as its leading coefficient (positive in this case), provided its roots are complex conjugate in pairs. This occurs when both the coefficients of the linear term and the discriminant of the cubic resolvent are negative (see, e.g., [7], pp. 119–125). Formulas (16) and (17) provide convenient algebraic representations of the said conditions.

So far the analysis has focused on a scalar random variable. Next it will be extended to the vector case by using the powerful argument of the so called spherical distributions (see “Appendix A2”). First we will devise the spherical representation of the CHS density that is a multivariate symmetric distribution, whose marginals are CHS densities, and then the same representation for its GC-like expansion. The following theorem establishes the form of a multivariate extension of a CHS density (SCHS henceforth) which depends on its modular variable (see “Appendix A2” for a definition of the latter). The second theorem proves that the GC-like expansion of the SCHS extension (GCSCHS hereafter) follows from the polynomial extension of the same modular variable. \square

Theorem 2 *The n -dimensional spherical extension of the CHS law, (SCHS) hereafter, has the representation*

$$g_n(\mathbf{x}) = \frac{2^{\frac{(n-3)}{2}} \pi^{\frac{n}{2}+1}}{\binom{\frac{n}{2}}{\binom{\frac{n}{2}+1}} \zeta(n-1)(2^{n+1}-1)} (\mathbf{x}'\mathbf{x})^{\frac{1}{2}} \left(\sin h \left(\frac{\pi}{\sqrt{2}} (\mathbf{x}'\mathbf{x})^{\frac{1}{2}} \right) \right)^{-1}, \quad (\mathbf{x}'\mathbf{x}) \in [0, \infty), \tag{19}$$

where $(z)_{(\theta)}$ and $\zeta(\cdot)$ denote the Pochhammer symbol and the Riemann zeta function, respectively.

Proof The spherical extension of a CHS density hinges on the density, f_R , of its modular variable, R , which, in turn, depends on the density generator (see formulas (72) and (74), “Appendix A2”). Now, taking

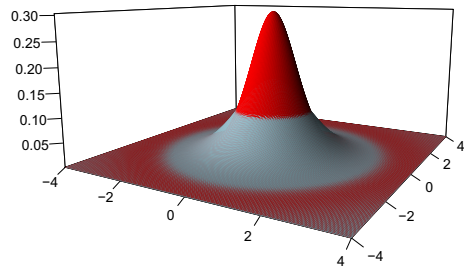
$$g(y) = y^{\frac{1}{2}} \left(\sin h \left(\frac{\pi}{\sqrt{2}} y^{\frac{1}{2}} \right) \right)^{-1}, \quad y \geq 0 \tag{20}$$

as the density generator, whose affiliation from the CHS density is apparent, and by using the following integral representation of the Riemann zeta function (see, e.g., [23] p. 348, 1980)

$$\zeta(\lambda) = \alpha^\lambda \Gamma^{-1}(\lambda) \frac{2^{\lambda-1}}{2^\lambda - 1} \int_0^\infty x^{\lambda-1} (\sin h(\alpha x))^{-1} dx, \tag{21}$$

where α and λ are positive parameters and $\Gamma(\cdot)$ is the Euler–Gamma function, simple computations yield the following expression for f_R

Fig. 1 SCHS (in dark) overlapped to the Gaussian law (in light)



$$f_R(r) = \frac{2^{\frac{(n-1)}{2}} r^n \pi^{n+1}}{\zeta(n+1)\Gamma(n+1)(2^{n+1}-1)} \left(\sin h\left(\frac{\pi}{\sqrt{2}}r\right) \right)^{-1}, r \in [0, \infty). \tag{22}$$

This, bearing in mind formulas (72) and (74) in “Appendix A2,” leads to (19). Trivially, $g_1(\mathbf{x})$ tallies with the CHS distribution. □

The graphs in Fig. 1 compare the (standard) bivariate Gaussian and the bivariate SCHS density. The SCHS (in dark) is overlapped to the Gaussian law (in light). As the SCHS density is more peaked and has fatter tails than the Gaussian law, the former distribution “covers” the peak and the tails of the latter. Conversely, the shoulders of the SCHS density, being slimmer than those of the Gaussian law, are covered by those of the latter density.

The issue of density reshaping, based on orthogonal polynomials, can be extended to n -dimensional spherical distributions. In fact, as in the univariate case, (even) moments of a spherical distribution can be properly modified by using ad hoc orthogonal polynomials with coefficients depending on the moments of the modular variable characterizing the spherical law.

The following theorem provides GC-like expansions of SCHS densities intended to model heavy-tailed multivariate series.

Theorem 3 *Let $g_n(\mathbf{x})$ be as in (19) and let $q_{n,4}(\mathbf{x}, \beta)$ be specified in terms of the vector argument $\mathbf{x}' = [x_1, x_2, \dots, x_n]$ as follows*

$$q_{n,4}(\mathbf{x}, \beta) = \left(1 + \frac{\beta}{\gamma_4} p_4\left((\mathbf{x}'\mathbf{x})^{\frac{1}{2}}\right) \right) \tag{23}$$

Here

$$p_4\left((\mathbf{x}'\mathbf{x})^{\frac{1}{2}}\right) = (\mathbf{x}'\mathbf{x})^2 - e(\mathbf{x}'\mathbf{x}) + g = ((\mathbf{x}'\mathbf{x})^{1/2})^4 - e((\mathbf{x}'\mathbf{x})^{1/2})^2 + g \tag{24}$$

is a second-order polynomial in the argument $(\mathbf{x}'\mathbf{x}) = r^2$, which can be read as a fourth-order (incomplete) orthogonal polynomial in the Euclidean norm $(\mathbf{x}'\mathbf{x})^{1/2} = r$. The coefficients e and g of this polynomial are based on the moments m_j

$$m_j = E(R^j) = \frac{\int_0^\infty y^{\frac{n+j}{2}-1} g(y) dy}{\int_0^\infty y^{\frac{n}{2}-1} g(y) dy}. \tag{25}$$

of the modular variable R and $\gamma_4 = \left\| p_4((\mathbf{x}'\mathbf{x})^{\frac{1}{2}}) \right\|$.

Furthermore, as $g_n(\mathbf{x})$ is spherical and $q_{n,4}(\mathbf{x}, \beta)$ is even, the product

$$\tilde{g}_n(\mathbf{x}, \beta) = q_{n,4}(\mathbf{x}, \beta) g_n(\mathbf{x}) \tag{26}$$

defines a family of GCSCHS densities with kurtosis increased by a quantity equal to

$$\tilde{\beta} = n^2 \frac{\beta}{(E(R)^2)^2} \tag{27}$$

with respect to that of the parent SCHS density.

Proof Following [22], the Mardia’s kurtosis index for a spherical variable is

$$K_n = n^2 \frac{E(R^4)}{(E(R^2))^2}. \tag{28}$$

According to (28), an increase in the kurtosis of a spherical variable can be attained by pushing up the fourth moment of the modular variable R that is by increasing the second moment of R^2 . □

Now, upon noting that, in light of (72) and (74), the density of a spherical variable is an even function in the argument $\|\mathbf{x}\|^2 = R^2$,

$$g_n(\mathbf{x}) = \frac{\Gamma\left(\frac{n}{2}\right)}{(\pi)^{\frac{n}{2}} \int_0^\infty y^{\frac{n}{2}-1} g(y) dy} g(\mathbf{x}'\mathbf{x}) = \frac{\Gamma\left(\frac{n}{2}\right)}{(\pi)^{\frac{n}{2}} \int_0^\infty y^{\frac{n}{2}-1} g(y) dy} g(\|\mathbf{x}\|^2), \tag{29}$$

the issue of density reshaping by means of orthogonal polynomials can be extended to n dimensional spherical distributions by using polynomials in the variable $\|\mathbf{x}\|^2$; in other words orthogonal polynomials associated with the density of R^2 , $f_{R^2}(r)$ hereafter. In this connection observe that, in light of the following relationship

$$f_R(r) = 2r f_{R^2}(r), \tag{30}$$

the density of a spherical variable can be directly expressed in terms of $f_{R^2}(r)$ as follows

$$g_n(\mathbf{x}) = 2rk f_{R^2}\left((\mathbf{x}'\mathbf{x})^{1/2}\right). \tag{31}$$

Accordingly, the GC-like expansions of $g_n(\mathbf{x})$ can be obtained by reshaping the density $f_{R^2}(r)$ with a binomial $q_{n,2}(r^2, \beta)$ in the argument r^2 that is

$$f_{\tilde{R}^2}(r, \beta) = q_{n,2}(r^2, \beta)f_{R^2}(r) \tag{32}$$

where $q_{n,2}(r^2, \beta) = \left(1 + \frac{\beta}{\gamma_2}p_2(r^2)\right)$ and $p_2(r^2) = (r^2)^2 - er^2 + g$. It is worth noting that, because R^2 is an asymmetric variable, $p_2(r^2)$ is a complete second-order polynomial in the variable r^2 .

According to formulas (64) and (67) in ‘‘Appendix A2,’’ the coefficients, e and g , of the second-order polynomial $p_2(r^2)$ can be expressed in terms of the moments \tilde{m}_j of the variable R^2 as follows

$$e = \frac{M_{3,2}}{M_{3,3}} = \frac{\tilde{m}_3\tilde{m}_0 - \tilde{m}_1\tilde{m}_2}{\tilde{m}_2\tilde{m}_0 - \tilde{m}_1^2}, \quad g = \frac{M_{3,1}}{M_{3,3}} = \frac{\tilde{m}_3\tilde{m}_1 - \tilde{m}_2^2}{\tilde{m}_2\tilde{m}_0 - \tilde{m}_1^2}. \tag{33}$$

Taking into account that $\tilde{m}_0 = 1$, the above coefficients can be expressed in terms of the moments, m_j , of the modular variable R as follows

$$e = \frac{m_6 - m_2m_4}{m_4 - m_2^2}, \quad g = \frac{m_6m_2 - m_4^2}{m_4 - m_2^2} \tag{34}$$

upon noting that $\tilde{m}_j = m_{2j}$. As a similar argument applies to the coefficient γ_2 , hence, the following identity

$$q_{n,2}(r^2, \beta) = q_{n,4}(r, \beta), \tag{35}$$

with $q_{n,4}(r, \beta)$ as specified in (23), holds true.

In light of the above result, simple computations prove that the spherical variable defined in terms of the reshaped modular variable \tilde{R}

$$\hat{g}_n(\mathbf{x}) = kf_{\tilde{R}}\left((\mathbf{x}'\mathbf{x})^{1/2}\right) \tag{36}$$

tallies with the GC-like expansion (26). In fact, taking into account (72), (30), (31) and (35), some computations yield

$$\hat{g}_n(\mathbf{x}) = kf_{\tilde{R}}\left((\mathbf{x}'\mathbf{x})^{1/2}\right) = 2rkf_{\tilde{R}^2}\left((\mathbf{x}'\mathbf{x})^{1/2}\right) \tag{37}$$

$$= 2rkq_{n,2}(r^2, \beta)f_{R^2}\left((\mathbf{x}'\mathbf{x})^{1/2}\right) = 2rkq_{n,4}(r, \beta)f_{R^2}\left((\mathbf{x}'\mathbf{x})^{1/2}\right) \tag{38}$$

$$= kq_{n,4}(r, \beta)f_R\left((\mathbf{x}'\mathbf{x})^{1/2}\right) = \tilde{g}_n(\mathbf{x}, \beta). \tag{39}$$

It follows that the GC-like expansion $\tilde{g}_n(\mathbf{x}, \beta)$ can be obtained by reshaping the modular variable R with the binomial $q_{n,4}(r, \beta)$. According to (34), the coefficients of the polynomial $p_4(\mathbf{x}'\mathbf{x})^{1/2}$ characterizing this binomial are functions of the moments of R as specified in (25), and proved in Theorem 3 on page 349 in [22].

Table 1 Descriptive statistics of standardized daily returns

Return	n	Min	Max	K	α	β	JB
$\wedge N225$	1480	- 7.3611	3.9015	6.2852	- 0.4265	2.2852	0.0000
$\wedge STOXX50E$	1542	- 4.2841	7.1949	6.3236	0.1483	2.3236	0.0000
$FTSEMIB.MI$	1547	- 3.9956	6.6057	5.4240	- 0.0281	1.4240	0.0000

Here, n is the number of observations; Min and Max are, respectively, the minimum and the maximum value of the series; K is the kurtosis index, α the skewness index and β is the extra kurtosis index; and JB is the p value of the Jarque–Bera test

3 Application to Financial Returns Data

In the application which follows, we have considered three daily financial series: the Nikkei 225 index, the ESTX50 EUR P index and the FTSE MIB index. The returns from these series, computed as the difference between the adjusted closing prices of two consecutive periods, divided by the adjusted closing price of the first period, will be denoted by $\wedge N225$, $\wedge STOXX50E$ and $FTSEMIB.MI$, respectively, from now on. All these series are recorded from 2009/01/01 to 2014/12/31. The series at stake, as many others in finance, are emblematic of the presence of excess kurtosis and skewness which are impeding characteristics to refer to the Gaussian and other popular alternatives for risk evaluations. This provides a strong motivation for creating a new conduit. Indeed, looking for a distribution tailored to both the kurtosis and skewness of the observed data, as proposed in this paper, becomes mandatory for an effective and accurate diagnosis of financial risks. The series chosen to illustrate the performance of the CHS distribution exhibit kurtosis values, respectively, equal to 6.28, 6.32 and 5.42 and skewness values, respectively, equal to - 0.42, 0.14 and 0.02 for which a Gaussian hypothesis is untenable. Likewise for the multivariate case: the Mardia's kurtosis indexes of the bivariate series ($\wedge N225, \wedge STOXX50E$), ($\wedge N225, FTSEMIB.MI$) and ($\wedge STOXX50E, FTSEMIB.MI$) are 15.48, 14.54 and 12.74, respectively, and are much greater than the kurtosis (8) of a bivariate Gaussian law. As such, these series provide an indicative case to show the effectiveness of GC-like expansions of both CHS and SCHS distributions in fitting the observed returns and in duly determining some risk measures, specifically value at risk (Var) and expected shortfall (ES). Let's start with an analysis focused on univariate financial series.

3.1 Univariate Approach

Table 1 reports the main descriptive statistics of all series.

As we can see, all data exhibit excess kurtosis and skewness. The Jarque–Bera test (JB) shows that the null hypothesis of normality is strongly rejected for all returns. Table 1 shows the estimates of the skewness and extra kurtosis, α and β , which have been obtained by using maximum likelihood (see “Appendix A3” for details). These estimates have been used to build GCCHS that have been fitted to the

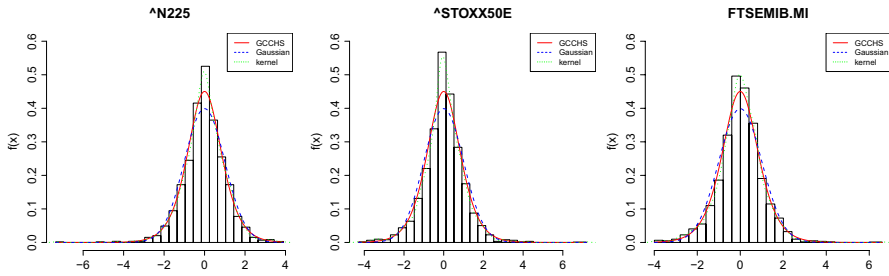


Fig. 2 Empirical distribution of $\hat{N225}$, $\hat{STOXX50E}$ and $FITSEMIB.MI$ returns approximated by GCCHS distribution (solid line), standardized normal distribution (dashed line) and kernel density (dotted line)

series. Figure 2 shows the Gaussian kernel densities¹ of the financial returns superimposed by their empirical distributions (the histogram of the empirical frequencies), the (standard) normal and the fitted GCCHS.

Figure 3 shows the QQplots of the quantiles of the financial returns against, respectively, the Gaussian (in the first column) and the GCCHS quantiles (in the second column).

In order to evaluate the goodness of fit of both GCCHS and Gaussian distributions to data, reference can be made to some indexes based on the absolute differences between the frequencies \hat{f}_i of the empirical kernels and the corresponding frequencies $f(x_i)$ estimated by using the GCCHS and the Gaussian densities, namely

$$A_1 = \frac{1}{2}h \sum_{i=1}^N |f(x_i) - \hat{f}_i| \tag{40}$$

$$A_2 = \frac{1}{N} \sum_{i=1}^N \frac{|f(x_i) - \hat{f}_i|}{\hat{f}_i + f(x_i)}. \tag{41}$$

In the above formulas, h represents the width of the histogram rectangles, \hat{f}_i is the height of the i -th rectangle and $f(x_i)$ is the ordinate of the GCCHS, or Gaussian distribution, at the midpoint of the basis of the i -th rectangle. The latter index has the advantage to be bounded that is

$$0 \leq A_2 \leq 1 \tag{42}$$

with the lower value corresponding to a perfect fit. The fit worsens as the index moves toward the upper bound. Table 2 gives the values taken by these indexes for

¹ The kernel densities have been estimated by using the command `density` in R software which, after scattering the probability mass of the empirical distribution on a regular grid, provides a linear approximation of the kernel.

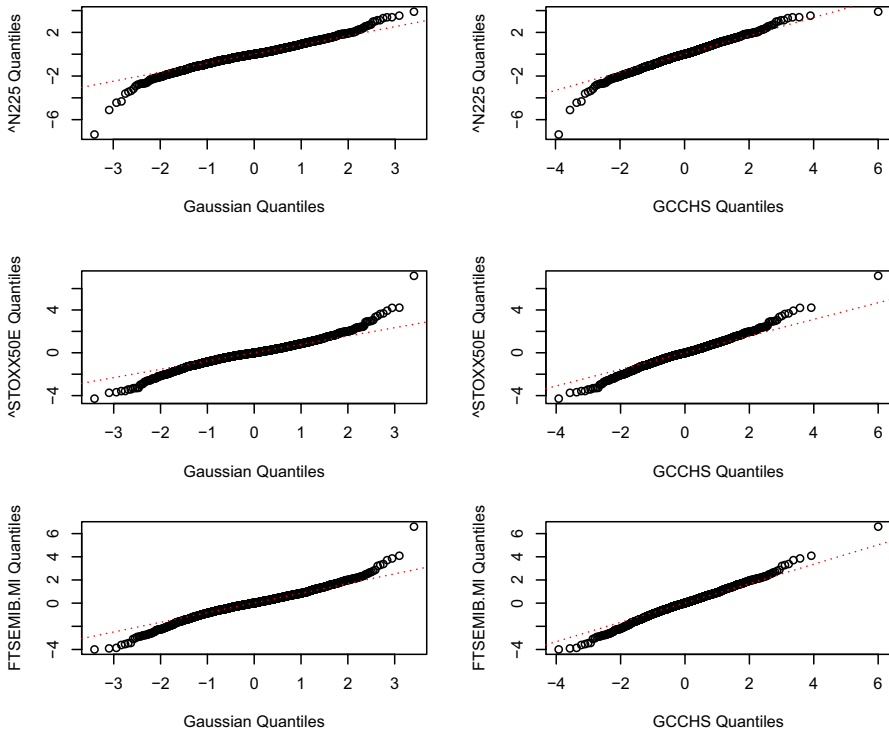


Fig. 3 QQplot of the empirical quantiles of $\wedge N225$, $\wedge STOXX50E$ and $FTSEMIB : MI$ returns against with the standardized normal quantiles (left column) and the GCCHS quantiles (right column)

Table 2 Values of the indexes A_1 and A_2 in the three returns

Return	A_1 Gaussian	A_1 GCCHS	A_2 Gaussian	A_2 GCCHS
$\wedge N225$	0.0807	0.0478	0.0020	0.0012
$\wedge STOXX50E$	0.1119	0.0478	0.0028	0.0012
$FTSEMIB.MI$	0.0981	0.0597	0.0025	0.0015

the series under examination which prove the better fit of GCCHS to data in comparison with the Gaussian law.

In order to gain a deeper insight into the effectiveness of the GCCHS distributions in fitting financial series, we have compared their performance with those of other distributions. These distributions are: the Gaussian, the Student- t , the Skew- t (see [16]), the normal inverse Gaussian, NIG (see [3]), the Fischer’s generalized hyperbolic density, GH, the generalized secant hyperbolic, GSH, and the skew generalized hyperbolic secant, SGSH (see e.g., [17]). All these distributions have been estimated via maximum likelihood with the functions fitdistrplus, and ghyp (for the NIG and GH) of the R *np* package. Table 3 reports the estimates of the parameters of all these distributions once fitted to returns.

Table 3 Parameter estimates for the fitted distributions

Parameter	$\wedge N225$	$\wedge STOXX50E$	$FTSEMIB.MI$
<i>Gaussian</i>			
μ	0	0	0
σ	1	1	1
<i>Student's t (γ)</i>			
γ	14.08	11.74	13.58
<i>Skew t ($\gamma; \lambda$)</i>			
γ	14.14	11.74	13.67
λ	0.9959	0.9961	0.9901
<i>Generalized secant hyperbolic (GSH) (λ)</i>			
λ	- 1.4234	-1.98330	- 1.6528
<i>Skew generalized secant hyperbolic (SGSH) ($\lambda; \gamma$)</i>			
λ	- 1.4232	- 1.9835	- 1.6517
γ	1.0004	0.9988	1.0016
<i>Normal inverse Gaussian (NIG) ($\mu; \sigma; \bar{\alpha}; \gamma$)</i>			
μ	0.0469	0.0180	0.0885
σ	0.9923	1.0031	0.9986
$\bar{\alpha}$	1.5433	0.8872	1.2406
γ	- 0.0729	- 0.0180	- 0.0884
<i>Generalized hyperbolic (GH) ($\mu; \sigma; \bar{\alpha}; \gamma; \lambda$)</i>			
μ	0.0469	- 0.01101	0.0792
σ	0.9923	0.9964	0.9975
$\bar{\alpha}$	0.4287	0.0003	0.9643
γ	- 0.0473	0.0110	- 0.0797
λ	1.7059	1.2563	0.8223

Then, the test for equality of univariate densities, proposed by [34], and based on metric entropy, has been implemented. The function `npunitest` in the *R np* package (see [25]) has been used for testing the null of equality of two densities. The test statistic is given by

$$S_\rho = \frac{1}{2} \int_{-\infty}^{\infty} \left(f(x)^{\frac{1}{2}} - g(x)^{\frac{1}{2}} \right)^2 dx \tag{43}$$

where $f(x)$ and $g(x)$ are the two densities being compared, that is, they are the kernel density of a return series and the corresponding fitting distribution, which is one of the aforementioned densities.² The test has been carried out for each of the three returns by assuming as a fitting distribution each of the densities introduced before (GCCHS, Gaussian, Student's *t*, Skew *t*, GSH, SGSH, NIG and GH distribution).

² The integral $\frac{1}{2} \int_{-\infty}^{\infty} \left(f(x)^{\frac{1}{2}} - g(x)^{\frac{1}{2}} \right)^2 dx$ is known as the Hellinger distance. Since it satisfies the triangular inequality, it is a proper measures of distance.

Table 4 The entropy measure S_ρ and corresponding p values (in brackets)

Return	GCCHS	Gaussian	Student's t	Skew t	GSH	SGSH	NIG	GH
$\wedge N225$	0.0057 (0.7875)	0.0600 (0.0500)	0.0493 (0.2424)	0.0495 (0.2828)	0.0049 (0.86)	0.0038 (0.1500)	0.0313 (0.8981)	0.0145 (0.9896)
$\wedge STOXX50E$	0.0032 (0.1625)	0.0760 (0.0000)	0.0562 (0.0707)	0.0568 (0.0404)	0.0042 (0.3900)	0.0034 (0.5100)	0.0289 (0.8717)	0.0381 (0.8934)
$FTSEMIB.MI$	0.0028 (0.2875)	0.0641 (0.0000)	0.0546 (0.0101)	0.0544 (0.0000)	0.0034 (0.2700)	0.0031 (0.4000)	0.0083 (0.7893)	0.01617 (0.7992)

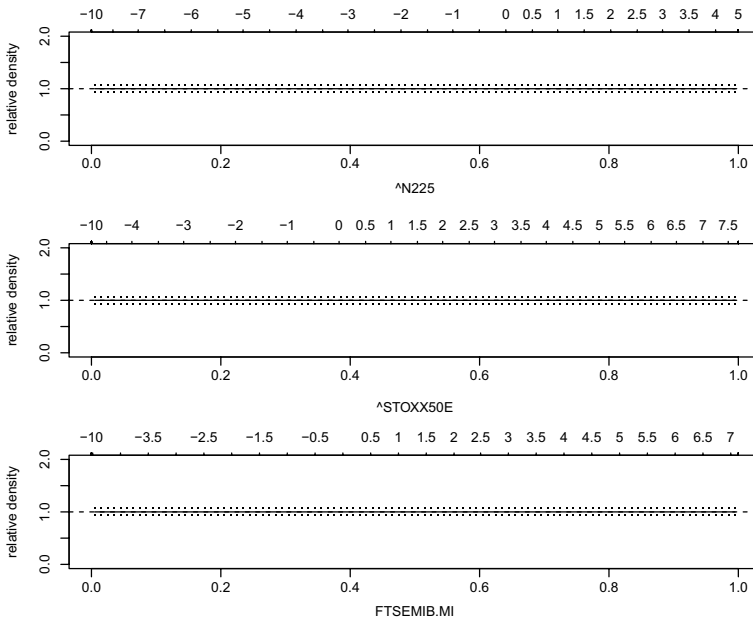


Fig. 4 Relative densities and confidence intervals for $\wedge N225$, $\wedge STOXX50E$ and $FTSEMIB : MI$ returns

Trivially, under the null hypothesis it is assumed that the two distributions are the same $S_\rho = 0$, otherwise $S_\rho > 0$. Table 4 displays the test statistics and the corresponding p values (in brackets) for the above mentioned distributions.

According to the results shown in Table 4, the null hypothesis cannot be rejected for the GCCHS, GSH, SGSH, NIG and GH distributions when $\alpha = 0.01$. This confirms that the empirical and the fitting distributions are not significantly different for these series.

To gain a better insight into the fitting of the GCCHS densities, we have also computed, for each of them, the relative densities with respect to their empirical counterpart (or kernel densities, see [24]). In our case, each relative density is the ratio between a given GCCHS density and a return kernel density, each evaluated in correspondence to the empirical quantiles. They have been estimated as in [24] with

the command *reldist* in the R *reldist* package. Since a relative density is distributed as a uniform variable, when the compared densities are identical, values of this distribution above (below) 1 provide evidence that the fitted distribution overestimate (underestimate) the frequency of the corresponding outcome. The graphs in Fig. 4 show these relative densities together with their 95% confidence intervals.

Looking at Fig. 4, we can see that GCCHS densities neither overestimate nor underestimate the kernel densities at hand. We can therefore draw the conclusion that the CHS distribution, once adjusted by its orthogonal polynomials, proves effective in fitting leptokurtic and skewed series.

The validity of a GCCHS distribution in computing some risk measures, like the value at risk (*VaR*) and the expected shortfall (*ES*), has been also evaluated. As is well known, *VaR* provides the minor loss we can expect to run within a certain period for a given probability (see [38]). The expected shortfall provides information about the size of losses exceeding *VaR*, namely the possible average loss (see [30]). Table 5 shows both *VaR* and *ES* estimates, computed at different significance levels α , by using GCCHS, Normal, Student *t*, Skew *t*, GSH, SGSH, NIG and GH densities. In this table, the estimated *VaR* and *ES* are compared with their corresponding empirical values. Empirical *VaR* has been computed as α -quantile of the empirical distribution, while the empirical *ES* as average of losses exceeding empirical *VaR*. Looking at Table 5, we see that GCCHS densities provide estimates of both *VaR* and *ES* that are very close to the empirical values.

Table 5 reports also the lower and upper bounds of percentage-bootstrap intervals (CI_{boot}) for VaR_{emp} and ES_{emp} , which have been built by selecting 10,000 bootstrap samples from the empirical density of each series. The results shown in this table confirm the validity of VaR_{α} and ES_{α} obtained by using GCCHS densities which never fall outside the bootstrap intervals for the corresponding empirical values. The same does not occur when these risk measures are computed via other densities.

3.2 Multivariate Approach

Finally, in order to evaluate the goodness of fit of GCSCHS densities in a multivariate context, we have considered three bivariate daily series: ($\wedge N225 - \wedge STOXX50E$), ($\wedge N225 - FTSEMIB.MI$) and ($FTSEMIB.MI - \wedge STOXX50E$). The scatter-plots of these series in the period 2009/01/01-2014/12/31 are reported in Fig. 5.

As in the univariate case, we have used the GCSCHS and the bivariate Student *t* densities in order to represent the empirical distributions. Table 6 shows the lengths, *N*, the Mardia's kurtosis indexes, *K*, of the bivariate GC-like expansions of these series and the degree of freedom of the bivariate Student's *t* distribution. Both these parameters have been estimated via the maximum likelihood method.

The function MVN of the R package has been used to evaluate the Mardia's multivariate kurtosis index. The parameters of the GCSCHS expansions have been estimated with the maximum likelihood.

To determine the log-likelihood function to be maximized, reference has been made to the density of an elliptical variable \mathbf{x}

Table 5 Risk measures on the univariate returns

	Emp	CJ_{boot}	Gaussian	GCCHS	Student's t	Skew t	GSH	SGSH	NIG	GH
Return	$\alpha = 0.1$									
$\wedge N225$										
<i>Var</i>	1.1641	(1.0925–1.2258)	1.2811	1.1400	1.3446	1.3526	1.1815	1.1822	1.1815	1.2915
<i>ES</i>	1.8395	(1.7482–1.9287)	1.7544	1.8822	1.9145	1.9389	1.8094	1.8103	1.8309	1.8265
$\wedge STOX50E$										
<i>Var</i>	1.1706	(1.0967–1.2263)	1.2811	1.1378	1.3580	1.3658	1.1383	1.2361	1.1329	1.1546
<i>ES</i>	1.8296	(1.7559–1.8921)	1.7544	1.8309	1.9502	1.9743	1.8258	1.8227	1.8347	1.9202
<i>FTSEMIB.MI</i>										
<i>Var</i>	1.1943	(1.1147–1.2915)	1.2811	1.1706	1.3471	1.3664	1.1677	1.1707	1.1747	1.1879
<i>ES</i>	1.8741	(1.8086–1.9410)	1.7544	1.8936	1.9210	1.9810	1.7155	1.8195	1.8651	1.8617
$\alpha = 0.05$										
$\wedge N225$										
<i>Var</i>	1.6409	(1.4997–1.7372)	1.6443	1.5976	1.7606	1.7698	1.6200	1.6209	1.6284	1.6415
<i>ES</i>	2.2976	(2.0978–2.5051)	2.0620	2.4253	2.2966	2.3649	2.2425	2.2436	2.2819	2.2610
$\wedge STOX50E$										
<i>Var</i>	1.6451	(1.5088–1.7952)	1.6443	1.5273	1.7856	1.7948	1.6085	1.6058	1.5996	1.6204
<i>ES</i>	2.2976	(2.1475–2.4712)	2.0620	2.3029	2.3499	2.4161	2.3060	2.3023	2.3313	2.2788
<i>FTSEMIBFTSEMIB.MI</i>										
<i>Var</i>	1.6486	(1.5414–1.8404)	1.6443	1.5827	1.7652	1.7876	1.6171	1.6208	1.6429	1.6575
<i>ES</i>	2.3373	(2.2313–2.4558)	2.0620	2.3337	2.3062	2.4730	2.2643	2.2688	2.34876	2.3272
$\alpha = 0.01$										
$\wedge N225$										
<i>Var</i>	2.6331	(2.1478–3.3576)	2.3256	2.9724	2.6225	2.6342	2.6216	2.6230	2.6749	2.6405
<i>ES</i>	3.6083	(2.9184–4.7212)	2.6643	3.8550	3.1290	3.6818	3.2408	3.2422	3.3510	3.2390
$\wedge STOX50E$										
<i>Var</i>	2.6831	(2.3584–3.2970)	2.3256	2.5371	3.6899	2.7025	2.7308	2.7267	2.7661	2.6811

Table 5 (continued)

	Emp	CI_{boot}	Gaussian	GCCHS	Student's t	Skew t	GSH	SGSH	NIG	GH
<i>ES</i>	3.3231	(3.0944–3.5599)	2.6643	3.3997	3.2398	3.7677	3.4387	3.4338	3.5634	3.3302
<i>FTSEMIB.MI</i>										
<i>VaR</i>	2.7466	(2.3621–3.0886)	2.3256	2.6068	2.6348	2.6640	2.6584	2.6636	2.7709	2.7351
<i>ES</i>	3.2361	(3.0003–3.4975)	2.6643	3.3744	3.1490	4.4814	3.3064	3.3123	3.5177	3.4025

Theoretical, empirical values of *VaR* and *ES* and the corresponding percentage-bootstrap interval. In bold are denoted values falling outside intervals

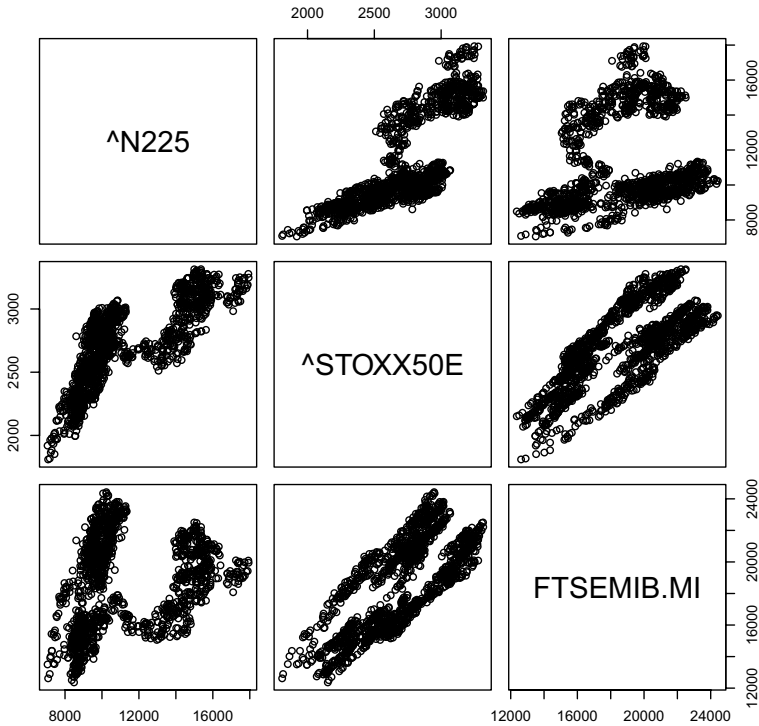


Fig. 5 Scatter-plots of the bivariate empirical returns $\wedge N225$, $\wedge STOXX50E$ and $FTSEMIB : MI$ returns

Table 6 Length (N), Mardia's kurtosis index, K , the parameter β of the GCSCHS density and the parameter ν of the Student's t distribution

Return	N	K	β	ν
$\wedge N225-\wedge STOXX50E$	1390	15.480	6.8109	11.8388
$\wedge N225-FTSEMIB.MI$	1395	14.5433	5.5485	13.2615
$\wedge STOXX50E-FTSEMIB.MI$	1521	12.746	3.1243	12.4738

$$\mathbf{x} = \boldsymbol{\mu} + \mathbf{V}'\mathbf{y} \tag{44}$$

where $\boldsymbol{\mu}$ denotes its mean vector, $\boldsymbol{\Sigma} = (\mathbf{V}'\mathbf{V})^{-1}$ its variance/covariance matrix and \mathbf{y} represents the spherical counterpart of \mathbf{x} . The density function of the latter variable is given by

$$g_n(\mathbf{x}) = c_n \det(\boldsymbol{\Sigma})^{-1/2} g((\mathbf{x} - \boldsymbol{\mu})' \boldsymbol{\Sigma}^{-1} (\mathbf{x} - \boldsymbol{\mu})) \tag{45}$$

where $c_n = \frac{\Gamma(\frac{n}{2})}{\pi^{n/2} \int_0^\infty y^{n/2-1} g(y) dy}$.

Accordingly, the log-likelihood function to be maximized with respect to $\boldsymbol{\mu}$, $\boldsymbol{\Sigma}$ and β turns out to be

$$l(\boldsymbol{\mu}, \boldsymbol{\Sigma}, \beta) = \sum_{t=1}^T \log f_t(\mathbf{x}_t, \boldsymbol{\mu}, \boldsymbol{\Sigma}, \beta) \quad (46)$$

where $f_t(\mathbf{x}_t, \boldsymbol{\mu}, \boldsymbol{\Sigma}, \beta)$, shortened in f_t , is given by

$$f_t = \left\{ 1 + \frac{\beta}{\gamma_4} p_4(q_t) \right\} g_n(q_t) \quad (47)$$

and

$$q_t = (\mathbf{x}_t - \boldsymbol{\mu})' \boldsymbol{\Sigma}^{-1} (\mathbf{x}_t - \boldsymbol{\mu}) = \text{tr}(\boldsymbol{\Sigma}^{-1} (\mathbf{x}_t - \boldsymbol{\mu})(\mathbf{x}_t - \boldsymbol{\mu})') \quad (48)$$

$$p_4(q_t) = q_t^2 - e q_t + g \quad (49)$$

Here the coefficients e , g , and γ_4 are as specified in Theorem 3. Furthermore, we have

$$g_n(q_t) = q_t \left(\sin h \left(\frac{\pi q_t}{\sqrt{2}} \right) \right) \quad (50)$$

To make the maximization of (46) unconstrained, in what follows $\boldsymbol{\Sigma} = (\mathbf{V}'\mathbf{V})^{-1}$ is meant to be the Cholesky decomposition of $\boldsymbol{\Sigma}$, so that the elements in the lower triangular matrix \mathbf{V} are free to move from minus to plus infinity. Moreover, for computational convenience, in order to bypass the inequality constraint (12), the scalar β in (47) has been parametrized as follows

$$\beta = \beta_{\max} \frac{1}{1 + \phi^2}, \quad (51)$$

where β_{\max} is the upper bound of β in (12) and ϕ is an unrestricted parameter.

Accordingly, the function (46) can be rewritten as

$$l = \sum_{t=1}^T \log \left(1 + \frac{\beta}{\gamma_4} p_4(q_t) \right) + \sum_{t=1}^T \log g_n(q_t), \quad (52)$$

Some computations (see ‘‘Appendix A3’’) show that the first-order conditions for the maximization of (52) are

$$\frac{\partial l}{\partial \boldsymbol{\mu}} = -2 \sum_{t=1}^T \boldsymbol{\Sigma}^{-1} (\mathbf{x}_t - \boldsymbol{\mu}) \gamma_t = \mathbf{0} \quad (53)$$

$$\frac{\partial l}{\partial \text{vech} \boldsymbol{\Sigma}} = -\mathbf{D}'_n (\boldsymbol{\Sigma}^{-1} \otimes \boldsymbol{\Sigma}^{-1}) \text{vec}(\mathbf{Z} - T \boldsymbol{\Sigma}) = \mathbf{0} \quad (54)$$

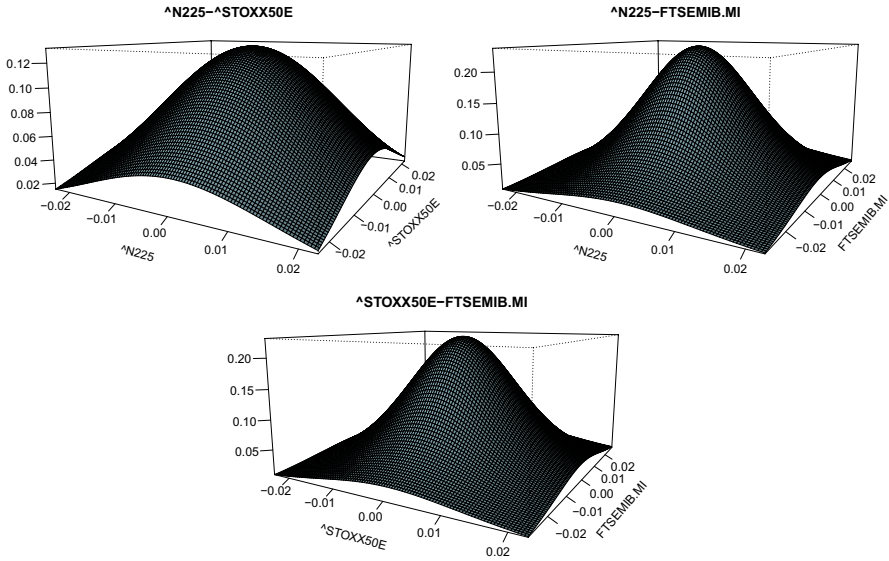


Fig. 6 GCSCHS densities fitted to the three bivariate series

$$\frac{\partial l}{\partial \phi} = - \sum_{t=1}^T \left(1 + \frac{\tilde{\beta}}{\gamma_4} p_4(q_t) \right)^{-1} \frac{p_4(q_t)}{\gamma_4} \beta_{\max} \frac{2\phi}{[1 + \phi^2]^2} = 0 \tag{55}$$

Here, $\gamma_t = \left(h_t + \left(1 + \frac{\beta}{\gamma_4} p_4(q_t) \right)^{-1} \frac{\beta}{\gamma_4} (2q_t - e) \right)$ where $h_t = \frac{1}{q_t} - \cot h\left(\frac{\pi q_t}{\sqrt{2}}\right) \frac{\pi}{\sqrt{2}}$, \mathbf{D}_n is the duplication matrix (see [32]), and $\mathbf{Z} = \sum_{t=1}^T (\mathbf{x}_t - \boldsymbol{\mu})(\mathbf{x}_t - \boldsymbol{\mu})' \gamma_t$.

The graphs in Fig. 6 show the GCSCHS densities fitted to the three bivariate series: $(\wedge N225- \wedge STOXX50E)$, $(\wedge N225-FTSEMIB.MI)$ and $(FTSEMIB.MI - \wedge STOXX50E)$.

Following [27], the VaR at a given level α , VaR_α , of a linear portfolio represented by a spherical variable \mathbf{r} , can be evaluated as follows

$$VaR_\alpha = q_{\alpha,n} \sqrt{\boldsymbol{\delta}' \boldsymbol{\Sigma} \boldsymbol{\delta}} \tag{56}$$

where $\boldsymbol{\delta}$ is a weighting vector that, in this case, is the unit vector and $\boldsymbol{\Sigma}$ is the variance/covariance matrix of \mathbf{r} . The scalar $q_{\alpha,n}$ is the unique positive solution of the transcendental equation

$$\alpha = \frac{2\pi^{\frac{n-1}{2}}}{\Gamma\left(\frac{n-1}{2}\right)} \int_{q_{\alpha,n}}^\infty \int_{z_1^2}^\infty (u - z_1^2)^{\frac{n-1}{2}} g_n(u) du dz_1, \tag{57}$$

where $g_n(u)$ is defined as in (26) and $\Gamma(\cdot)$ is the Euler–Gamma function.

According to (56), the theoretical ES at a given level α , (ES_α) , can be evaluated as follows

Table 7 Empirical VaR with associated percentage-bootstrap intervals and theoretical VaR computed with GCSCHS and Student t , VaR_{α}^{GC} and VaR_{α}^t

Returns	α	VaR_{e_1}	VaR_{e_2}	$CI_{boot}(VaR_{e_1})_{\alpha}$	VaR_{α}^{GC}	VaR_{α}^t
$\wedge N225- \wedge STOXX50E$	0.01	3.8542	3.6278	(3.0318–4.6149)	3.7359	3.7993
	0.05	2.3028	2.2813	(2.1264–2.4809)	2.2060	2.5234
	0.1	1.6231	1.6805	(1.5444–1.7410)	1.6276	1.9195
$\wedge N225- FTSEMIB.MI$	0.01	3.8803	3.5706	(3.0382–4.2823)	3.6898	3.7380
	0.05	2.3558	2.2859	(2.1121–2.4880)	2.2270	2.5007
	0.1	1.6399	1.7044	(1.5348–1.7272)	1.6476	1.9074
$\wedge STOXX50E- FTSEMIB.MI$	0.01	3.7720	3.7080	(3.3763–4.7502)	3.6149	3.7700
	0.05	2.3784	2.3122	(2.1367–2.5634)	2.2651	2.5126
	0.1	1.7208	1.7003	(1.5549–1.7081)	1.6855	1.9137

$$ES_{\alpha} = K_{ES} \sqrt{\delta' \Sigma \delta} \tag{58}$$

where

$$K_{ES} = \frac{\pi^{\frac{n-1}{2}}}{\alpha \Gamma\left(\frac{n+1}{2}\right)} \int_{q_{\alpha,n}^2}^{\infty} (u - q_{\alpha,n}^2)^{\frac{n-1}{2}} \tilde{g}_n(u, \beta) du. \tag{59}$$

As benchmarks for VaR_{α} and ES_{α} , we have evaluated the corresponding empirical measures in two different ways. Firstly, we have computed the empirical VaR as follows

$$VaR_{e_1} = \sqrt{VaR_1^2 + VaR_2^2 - 2cov(X_1, X_2)} \tag{60}$$

where VaR_j is the VaR of the j -th univariate series and $cov(\cdot)$ denotes the covariance of the bivariate series X_i, X_j . The function VARES of the R package has been used for this scope. Then, after computing the ES_j of each univariate series X_j by using VaR_{e_1} as the critical level, we have computed the empirical ES of the bivariate series as follows

$$ES_{e_1} = ES_1 + ES_2. \tag{61}$$

Other measures of empirical VaR and ES , VaR_{e_2} and ES_{e_2} hereafter, have been obtained by applying Kandem’s formulas (56) and (58) with $g_n(u)$ replaced by the empirical density of the bivariate series and $q_{\alpha,n}$ by the empirical quantile. Tables 7 and 8 compare both the theoretical values of these risk measures, VaR_{α}^{GC} and ES_{α}^{GC} , under the GCSCHS and the bivariate Student’s t models, VaR_{α}^t and ES_{α}^t , with the corresponding empirical values (VaR_{e_1}, VaR_{e_2}), and (ES_{e_1}, ES_{e_2}), respectively.

Just like in the univariate case, also in the bivariate case GCSCHS densities provide good estimates for both VaR and ES . Looking at Tables 7 and 8, we see that the estimates of these risk measures provided by GCSCHS densities are always close to the corresponding empirical values and they always lie inside the

Table 8 Empirical ES with associated percentage-bootstrap intervals and theoretical ES computed with GCSCHS and Student t , ES_{α}^{GC} and ES_{α}^t

Returns	α	ES_{e_1}	ES_{e_2}	$CI_{boot}(ES_{e_1})_{\alpha}$	ES_{α}^{GC}	ES_{α}^t
$\wedge N225- \wedge STOXX50E$	0.01	10.2197	9.5000	(4.5445–11.0215)	9.7810	9.1473
	0.05	6.1143	6.3431	(5.4950–6.9698)	6.3393	6.6388
	0.1	4.6465	5.1221	(4.3440–5.0704)	5.0532	5.5109
$\wedge N225- FTSEMIB.MI$	0.01	9.6302	9.2846	(4.0386–10.6990)	9.5533	8.9454
	0.05	6.2981	6.2710	(5.3995–6.9376)	6.3052	6.5417
	0.1	4.6596	5.1031	(4.3281–4.9788)	5.0572	5.4459
$\wedge STOXX50E- FTSEMIB.MI$	0.01	8.1508	9.2411	(5.7912–8.5969)	9.1050	9.0505
	0.05	5.8875	6.3621	(5.4456–6.3319)	6.2364	6.5924
	0.1	4.6811	5.1539	(4.3198–4.7627)	5.0622	5.4798

percentage-bootstrap intervals (CI_{boot}) built for VaR_{emp} and ES_{emp} by selecting 10,000 block bootstrap samples from the empirical density of each series. This is not true for the theoretical values under the Student’s t distribution. In particular, the VaR_{α}^t always overestimates the empirical values because it falls outside the bootstrap interval when $\alpha = 0.05$ and $\alpha = 0.1$. The ES_{α}^t follows the same trend as it falls always outside the bootstrap interval $\alpha = 0, 1$ and, in the case of the pair return ““STOXX50E-FTSEMIB.MI,” is always outside the percentage-bootstrap bounds for every α level. Hence, we can draw the conclusion that GCSCHS densities provide precautionary estimates of the risk measures here considered.

4 Conclusion

This paper proposes a family of leptokurtic distributions obtained via a polynomial transformation of a leptokurtic density, called convoluted hyperbolic secant (CHS). The CHS density shares several desirable properties with the logistic and hyperbolic secant laws, to which it is connected by some intriguing relationships. Reshaping the CHS by using its own orthogonal polynomials yields Gram–Charlier-like expansions (GCCHS) able to account for skewness and kurtosis found in empirical data. The multivariate extension of both CHS and its GCCHS expansions (GCSCHS) can be obtained on a spherical distribution argument. The possibility of encoding both excess kurtosis and skewness, by using the orthogonal polynomial technique, makes GCCHS densities and their spherical version, a valuable resource for modeling financial asset return distributions. This considerably broadens the application domain of the previous approach based on the transformation of the Gaussian law by Hermite polynomials (see e.g., [43]). An application to empirical financial returns data provides practical evidence of the effectiveness of the proposed densities to fit both univariate and multivariate leptokurtic, skewed distributions. The capability of both GCCHS and GCSCHS densities in assessing some risk measures, like the value at risk and the expected shortfall, is also evaluated and leads to the conclusion that they are more effective than standard alternatives considered by the extant literature.

Appendix

A1: Orthogonal Polynomials

A sequence of polynomials

$$p_n(x) = x^n + a_{n-1}x^{n-1} + a_{n-2}x^{n-2} + \dots + a_0 \tag{62}$$

where a_0, a_1, \dots, a_{n-1} are reals and n is a nonnegative integer, is orthogonal with respect to a density function $f(x)$ with finite moments if the following holds

$$\int_{-\infty}^{\infty} p_n(x)p_d(x)f(x)dx = \gamma_n\delta_{nd}, \quad d = 0, 1, \dots, n - 1, \quad n \in N \cup \{0\}. \tag{63}$$

Here $\gamma_n > 0$, δ_{nd} is the Kronecker symbol ($\delta_{nd} = 1$ if $n = d$, and zero otherwise) and $p_0(x) = 1$ by convention. Condition (63) determines $p_n(x)$. The coefficients a_0, a_1, \dots, a_{n-1} of $p_n(x)$ are functions of the moments m_j of the density $f(x)$

$$a_j = (M_{n+1,n+1})^{-1}M_{n+1,j+1}, \tag{64}$$

where $M_{n+1,i}$ is the cofactor of the $(n + 1, i)$ entry of the $(n + 1, n + 1)$ moment matrix

$$\begin{bmatrix} m_0 & m_1 & m_2 & \dots & m_n \\ \vdots & \vdots & \vdots & & \vdots \\ m_{n-1} & m_n & m_{n+1} & \dots & m_{2n-1} \\ 1 & x & x^2 & \dots & x^n \end{bmatrix}. \tag{65}$$

The quantity γ_n is given by

$$\gamma_n = \frac{M_{n+2,n+2}}{M_{n+1,n+1}}, \tag{66}$$

where reference is made to a moment matrix of dimensions $(n + 2, n + 2)$ (see, e.g., [12, 41]).

For even densities, odd moments are null and orthogonal polynomials $p_n(x)$ are even functions if n is even, and odd otherwise (see [41]). In particular, the third and fourth-order orthogonal polynomials associated with an even density $f(x)$ turn out to be of the form

$$p_3(x) = x^3 - dx, \quad p_4(x) = x^4 - ex^2 + g, \tag{67}$$

where d, g and e are functions of moments of the random variable x .

For our purposes, the following trinomial

$$q(x, \alpha, \beta) = 1 + \frac{\alpha}{\gamma_3}p_3(x) + \frac{\beta}{\gamma_4}p_4(x) \tag{68}$$

is of particular interest because it can be used to alter the third and fourth moments of $f(x)$ to an extent equal to α and β , respectively. To this end, consider the function

$$\tilde{g}(x, \alpha, \beta) = q(x, \alpha, \beta)f(x), \quad (69)$$

where $(q(x, \alpha, \beta))$ is subject to be positive. The function $\tilde{g}(x, \alpha, \beta)$ is called Gram–Charlier-like (GC-like) expansion of $f(x)$. The following theorem proves a fundamental result on moments of GC-like expansions defined as in (69).

Theorem A1 *The moments μ_j up to the 4-th order of the GC-like expansion in (69) are related to the moments m_j of the parent density $f(x)$ as follows*

$$\begin{cases} \mu_j = m_j & \text{for } j < 3 \\ \mu_j = m_j + \alpha & \text{for } j = 3 \\ \mu_j = m_j + \beta & \text{for } j = 4. \end{cases} \quad (70)$$

Higher moments of $\tilde{g}(x, \alpha, \beta)$ turn out to be algebraic functions of the moments of $f(x)$.

Proof The proof follows from the properties of orthogonal polynomials as shown in [14, 43]. \square

A2: Spherical Distributions

Spherical distributions and the corresponding random vectors are also called “radial” (see [29]), or “isotropic” (see [5]), because they correspond to the class of rotationally symmetric distributions. Accordingly, any spherical random vector admits a stochastic representation of the form

$$\mathbf{x} = R\mathbf{U}^{(n)}, \quad (71)$$

where $\mathbf{U}^{(n)}$ is a random vector uniformly distributed on the unit hypersphere with $n-1$ topological dimensions and $R = (\mathbf{x}'\mathbf{x})^{\frac{1}{2}}$ is a nonnegative random variable, called modular variable, independent of $\mathbf{U}^{(n)}$. An interesting property of spherical distributions is that their densities may be expressed via the density function of the modular variable, provided it is absolutely continuous.

Theorem A2 *An n -dimensional spherical random vector \mathbf{x} has a density, $g_n(\mathbf{x})$, of the form*

$$g_n(\mathbf{x}) = kf_R\left((\mathbf{x}'\mathbf{x})^{\frac{1}{2}}\right), \quad (72)$$

where f_R is the density of the modular variable $R = (\mathbf{x}'\mathbf{x})^{\frac{1}{2}}$,

$$k = \frac{\Gamma\left(\frac{n}{2}\right)}{2(\pi)^{\frac{n}{2}}}r^{1-n} \quad (73)$$

and $\Gamma(\cdot)$ is the Euler–Gamma function. Furthermore, the density f_R has the integral representation

$$f_R(r) = \frac{2r^{n-1}}{\int_0^\infty y^{\frac{n}{2}-1} g(y) dy} g(r^2) \tag{74}$$

in terms of a nonnegative Lebesgue measurable function $g(\cdot)$ called density generator.

Proof For the proof see [15, 22]. □

A3: Maximum Likelihood Estimation of GCSCHS Laws

In the univariate case, in light of (5), the log-likelihood function to maximize is

$$\sum_{i=1}^N l_i \tag{75}$$

were

$$l_i = \log(q(x_i, \mu, \sigma, \alpha, \beta)) + \log f(x_i) \tag{76}$$

and

$$q(x_i, \mu, \sigma, \alpha, \beta) = \left(1 + \frac{\alpha}{\gamma_3} p_3(\tilde{x}_i) + \frac{\beta}{\gamma_4} p_4(\tilde{x}_i) \right) \tag{77}$$

with \tilde{x}_i denoting the standardized variable: $\tilde{x}_i = \frac{x_i - \mu}{\sigma}$.

In the multivariate case, bearing in mind (47), the log-likelihood function is as in (75) with l_i specified as follows where

$$l_i = \log f_i = \log g_n(q_i) + \log \left(1 + \frac{\beta}{\gamma_4} p_4(q_i) \right) \tag{78}$$

and q_i , $p_4(q_i)$, $g_n(q_i)$ and β are defined as in (48), (49), (45) and (51), respectively. In the latter case, the procedure to obtain the maximum likelihood estimate of μ , $\text{vech}(\Sigma)$ and v , hinges on the gradient vector

$$\xi = \frac{\partial l_i}{\partial \theta} \tag{79}$$

and the Hessian matrix

$$\mathbf{H} = \frac{\partial^2 l_i}{\partial \theta \partial \theta'} = \frac{\partial \xi}{\partial \theta'} \tag{80}$$

where

$$\theta' = [\boldsymbol{\mu}', \text{vech}(\boldsymbol{\Sigma})', \phi] \tag{81}$$

As for the gradient, we need the following derivatives

$$\frac{\partial \log \tilde{g}_n(q_t)}{\partial \boldsymbol{\mu}} \tag{82}$$

$$\frac{\partial \log \tilde{g}_n(q_t)}{\partial \text{vech} \boldsymbol{\Sigma}} \tag{83}$$

$$\frac{\partial \log \left(1 + \frac{\tilde{\beta}}{\gamma_4} p_4(q_t) \right)}{\partial \boldsymbol{\mu}} \tag{84}$$

$$\frac{\partial \log \left(1 + \frac{\tilde{\beta}}{\gamma_4} p_4(q_t) \right)}{\partial \text{vech} \boldsymbol{\Sigma}} \tag{85}$$

$$\frac{\partial \log \left(1 + \frac{\tilde{\beta}}{\gamma_4} p_4(q_t) \right)}{\partial \phi} \tag{86}$$

where

$$g(q_t) = q_t \left(\sin h \left(\frac{\pi q_t}{\sqrt{2}} \right) \right)^{-1}. \tag{87}$$

As far as derivatives (82) and (83) are concerned, some computations yield

$$\frac{\partial \log \tilde{g}_n(q_t)}{\partial \boldsymbol{\mu}} = \frac{\partial \log g(q_t)}{\partial \boldsymbol{\mu}} = \frac{\partial \log g(q_t)}{\partial q_t} \frac{\partial q_t}{\partial \boldsymbol{\mu}} = -2 \boldsymbol{\Sigma}^{-1} (\mathbf{x}_t - \boldsymbol{\mu}) h_t \tag{88}$$

$$\frac{\partial \log \tilde{g}_n(q_t)}{\partial \text{vech} \boldsymbol{\Sigma}} = -\frac{1}{2} \frac{\partial \log |\boldsymbol{\Sigma}|}{\partial \text{vech} \boldsymbol{\Sigma}} + \frac{\partial \log g(q_t)}{q_t} \frac{\partial(q_t)}{\text{vech} \boldsymbol{\Sigma}} = -\frac{1}{2} \mathbf{D}'_n \text{vec} \boldsymbol{\Sigma}^{-1} - h_t \mathbf{D}'_n \text{vec} \mathbf{G}_t, \tag{89}$$

where \mathbf{D}_n denotes the duplication matrix (see [32]), $\mathbf{G}_t = \boldsymbol{\Sigma}^{-1} (\mathbf{x}_t - \boldsymbol{\mu})(\mathbf{x}_t - \boldsymbol{\mu})' \boldsymbol{\Sigma}^{-1}$, and

$$h_t = \frac{\partial \log g(q_t)}{\partial q_t} = (g(q_t))^{-1} \frac{\partial g(q_t)}{q_t} = \frac{1}{q_t} - \cot h \left(\frac{\pi q_t}{\sqrt{2}} \right) \frac{\pi}{\sqrt{2}} \tag{90}$$

Equations (88) and (89) have been worked out upon noting that

$$\frac{\partial q_t}{\partial \boldsymbol{\mu}} = -2 \boldsymbol{\Sigma}^{-1} (\mathbf{x}_t - \boldsymbol{\mu}) \tag{91}$$

$$\frac{\partial \log |\Sigma|}{\partial \text{vech} \Sigma} = \left\{ \frac{\partial \log |\Sigma|}{\partial \text{vec} \Sigma'} \frac{\partial \text{vec} \Sigma}{\partial \text{vech} \Sigma'} \right\}' = \mathbf{D}'_n \text{vec} \Sigma^{-1} \tag{92}$$

$$\frac{\partial q_t}{\partial \text{vech} \Sigma} = \left\{ \frac{\partial q_t}{\partial \text{vec} \Sigma'} \frac{\partial \text{vec} \Sigma}{\partial \text{vech} \Sigma'} \right\}' = -\mathbf{D}'_n \text{vec} \mathbf{G}_t. \tag{93}$$

Derivatives (84) and (85) turn out to be

$$\frac{\partial \log \left(1 + \frac{\tilde{\beta}}{\gamma_4} p_4(q_t) \right)}{\partial \boldsymbol{\mu}} = \left(1 + \frac{\tilde{\beta}}{\gamma_4} p_4(q_t) \right)^{-1} \frac{\partial \left(1 + \frac{\tilde{\beta}}{\gamma_4} p_4(q_t) \right)}{\partial q_t} \frac{\partial q_t}{\partial \boldsymbol{\mu}} = 2\lambda_t \Sigma^{-1} (\mathbf{x}_t - \boldsymbol{\mu}) \tag{94}$$

$$\frac{\partial \log \left(1 + \frac{\tilde{\beta}}{\gamma_4} p_4(q_t) \right)}{\partial \text{vech} \Sigma} = \left(1 + \frac{\tilde{\beta}}{\gamma_4} p_4(q_t) \right)^{-1} \frac{\partial \left(1 + \frac{\tilde{\beta}}{\gamma_4} p_4(q_t) \right)}{\partial q_t} \frac{\partial q_t}{\partial \text{vech} \Sigma} = \lambda_t \mathbf{D}'_n \text{vec} \mathbf{G}_t, \tag{95}$$

where $\lambda_t = -\left(1 + \frac{\tilde{\beta}}{\gamma_4} p_4(q_t) \right)^{-1} \frac{\tilde{\beta}}{\gamma_4} (2q_t - e)$.

Derivatives (94) and (95) have been computed by taking in to account (91)–(93), as well as

$$\frac{\partial p_4(q_t)}{\partial q_t} = (2q_t - e). \tag{96}$$

Lastly, derivative (86) is given by

$$\frac{\partial \log \left(1 + \frac{\tilde{\beta}}{\gamma_4} p_4(q_t) \right)}{\partial \phi} = \left(1 + \frac{\tilde{\beta}}{\gamma_4} p_4(q_t) \right)^{-1} \frac{\partial \left(1 + \frac{\tilde{\beta}}{\gamma_4} p_4(q_t) \right)}{\partial \tilde{\beta}} \frac{\partial \tilde{\beta}}{\partial \phi} = d_t \frac{2\phi}{(1 + \phi^2)^2} \tag{97}$$

where $d_t = -\left(1 + \frac{\tilde{\beta}}{\gamma_4} p_4(q_t) \right)^{-1} \frac{p_4(q_t)}{\gamma_4} \beta_{max}$.

Second-order derivatives, necessary to obtain the Hessian matrix, can be worked out by using the procedure so far followed.

References

1. Adcock CJ, Shutes K (2012) On the multivariate extended skew-normal, normal-exponential, and normal-gamma distributions. *J Stat Theory Pract* 6–4:636–664
2. Barakat MH (2015) A new method for adding two parameters to a family of distributions with applications to the normal and exponential families. *Stat Methods Appl* 24(3):359–372
3. Barndorff-Nielsen O, Blæsild P (1983) Hyperbolic distributions. In: Johnson NL, Kotz S, Read CB (eds) *Encyclopedia of statistical sciences*, vol 3. Wiley, New York
4. Baten WD (1934) The probability law for the sum of n independent variables, each subject to the law $((1/2h)\text{sech}(\pi x/(2h)))$. *Bull Am Math Soc* 40:284–290
5. Bingham NH, Kiesel R (2002) Semi-parametric modelling in finance: theoretical foundations. *Quant Finance* 2(4):241–250

6. Bracewell RN (1986) The Fourier transform and its application. Mc Graw Hill, New York
7. Bronshtein IN, Semendiyayev KA, Musiol G, Muhlrig H (1998) Handbook of mathematics. Springer, Berlin
8. Carreau J, Bengio Y (2009) A hybrid Pareto model for asymmetric fat-tailed data: the univariate case. *Extremes* 12:53–76. <https://doi.org/10.1007/s10687-008-0068-0>
9. Carreau JP, Naveau P, Sauquet E (2009) A statistical rainfall-runoff mixture model with heavy-tailed components. *Water Resour Res* 45:W10437. <https://doi.org/10.1029/2009WR007880>
10. Carreau J, Vrac M (2011) Stochastic down scaling of precipitation with neural network conditional mixture models. *Water Resour Res* 47:W10502. <https://doi.org/10.1029/2010WR010128>
11. Cheah PK, Fraser DAS, Reid N (1993) Some alternatives to Edgeworth. *Can J Stat* 21(II):131–138
12. Chihara TS (1978) An introduction to orthogonal polynomials. Gordon & Breach, New York
13. Cooley D, Nychka D, Nevada P (2007) Bayesian spatial modeling of extreme precipitation return levels. *J Am Stat Assoc* 102(479):824–840
14. Faliva M, Poti' V, Zoia MG (2016) Orthogonal polynomials for tailoring density functions to excess kurtosis, asymmetry and dependence. *Commun Stat Theory Methods* 45:49–62
15. Fang KT, Kotz S, Ng KW (1990) Symmetric multivariate and related distributions. Chapman and Hall, London
16. Fernandez C, Steel MF (1998) On Bayesian modeling of fat tails and skewness. *J Am Stat Assoc* 93:359–371
17. Fisher MJ (2013) Generalized hyperbolic secant distribution with application to finance. Springer, Berlin
18. Frigessi A, Haug O, Rue H (2002) A dynamic mixture for unsupervised tail estimation without threshold selection. *Extremes* 5:219–235
19. Johnson NL, Kotz S, Balakrishnan N (1994) Continuous univariate distributions. Wiley, New York
20. García CB, van García Perez J, Dorp JR (2011) Modelling heavy-tailed, skewed and peaked uncertainty phenomena with bounded support. *Stat Methods Appl* 20:463–486
21. Genton MG (2004) Skew-symmetric and generalized skew-elliptical distributions. In: Genton MG (ed) *Skew-elliptical distributions and their applications*. Chapman and Hall, London, pp 101–120
22. Gomez E, Gomez-Villegas MA, Marin JM (2003) A survey on continuous elliptical vector distributions. *Rev Mat Complut* 16(1):345–361
23. Gradshteyn IS, Ryzhik IM (1980) Table of integrals, series and products. Academic Press, London
24. Handcock MS (2014) Relative distribution methods. Version 1.6-3. Project home page at <http://www.stat.ucla.edu/~handcock/ReID> ist <http://CRAN.R-project.org/package=reldist>
25. Hayfield T, Racine JS (2008) Nonparametric econometrics: the np package. *J Stat Softw* 27(5):1–32
26. Jondeau E, Rockinger M (2001) Gram–Charlier densities. *J Econ Dyn Control* 25(10):1457–1483
27. Kandem JS (2005) Value at risk and expected shortfall for linear portfolios with elliptically distributed risk factors. *J Theor Appl Finance* 8:537–551
28. Katz R, Parlange M, Naveau P (2002) Extremes in hydrology. *Adv Water Resour* 25:1287–1304
29. Kelker D (1970) Distribution theory of spherical distributions and a location-scale parameter generalization. *Sankhyā*. Indian J Stat Series A:419–430
30. Landsman Z, Valdez AE (2004) Tail conditional expectations for elliptical distributions. *N Am Actuar J* 8(3):118–122
31. Li C, Singh VP, Mishra AK (2012) Simulation of the entire range of daily precipitation using a hybrid probability distribution. *Water Resour Res* 48:W03521. <https://doi.org/10.1029/2011WR011446>
32. Lutkepohl H (1996) Handbook of matrices. Wiley, Hoboken
33. MacDonald A, Scarrot, Lee D, Darlow B, Reale M, Russel G (2011) A flexible extreme value mixture model. *Comput Stat Data Anal* 55:2137–2157
34. Maasoumi E, Racine J (2002) Entropy and predictability of stock market returns. *J Econom* 107(1):291–312
35. Mills TC (1999) The econometric modelling of financial time series. Cambridge University Press, Cambridge
36. Naveau P, Toreti I, Koplaki E (2014) A fast nonparametric spatio-temporal regression scheme for generalized Pareto distributed heavy precipitation. *Water Resour Res* 50:4011–4017. <https://doi.org/10.1002/2014WR015431>
37. Papastahopoulos I, Tawn AJ (2013) Extended generalized Pareto models for tails estimation. *J Stat Plan Inference* 143:131–143

38. Philippe J (2001) Value at risk: the new benchmark for managing financial risk. McGraw-Hill Professional, New York
39. Rachev ST, Hoechstoeetter M, Fabozzi FJ (2010) Probability and statistics for finance. Wiley, New York
40. Ruppert D, Wand MP (1992) Correcting for kurtosis in density estimation. *Aust N Z J Stat* 34(I):19–29
41. Szego G (1967) Orthogonal polynomials. American Mathematical Society Colloquium Publications, vol. 23, American Mathematical Society, New York, 1939, 3rd edn
42. Szego G (2004) Risk measures for the 21 century. Wiley, New York
43. Zoia M (2010) Tailoring the Gaussian law for excess kurtosis and asymmetry by Hermite polynomials. *Commun Stat Theory Methods* 39:52–64

Publisher's Note Springer Nature remains neutral with regard to jurisdictional claims in published maps and institutional affiliations.